

# Deformation Characteristics of Granular Materials in Cyclic One-Dimensional Loading Tests

Junichi Koseki · Tomonori Mikami · Takeshi Sato

Accepted: 7 January 2014 / Published online: 28 January 2014  
© Springer New York 2014

**Abstract** In order to study deformation characteristics of geomaterials under simulated traffic loading conditions, a series of cyclic one-dimensional loading tests was conducted on compacted specimens with varied heights, which were made from four types of granular materials consisting of particles with a mean diameter in the range of 2.2 to 5.8 mm. By assuming that the top and bottom ends of the specimen were affected by the bedding error, it was attempted to estimate the residual strain after cyclic loading and the constrained modulus during cyclic loading of the tested specimens, which are free from the effects of bedding error. As a result, the residual strains of the tested materials were on the order of 0.1 %, while much higher residual strains were estimated for the layers affected by the bedding error. In addition, the estimated values of the constrained modulus were much larger than their nominal values that were evaluated in a conventional manner. With one type of the tested material, however, reasonable estimation could not be made, suggesting a limitation of the simplified assumption. The estimated values of the residual strain of the normal layer and the constrained moduli were consistent with the results from relevant triaxial tests.

**Keywords** Cyclic one-dimensional loading test · Residual deformation · Constrained modulus · Bedding error · Triaxial test · Local deformation measurement

## Introduction

In evaluating experimentally the performance of geomaterials to be employed for road and railway bases against traffic loading, resilient modulus tests using triaxial apparatus

---

J. Koseki (✉)  
University of Tokyo, Tokyo, Japan  
e-mail: koseki@iis.u-tokyo.ac.jp

T. Mikami  
Kajima Corporation, Tokyo, Japan

T. Sato  
Integrated Geotechnology Institute Limited, Tokyo, Japan

have been widely conducted ([1, 3, 9, 10] among others). In conducting these tests, cyclic loading is applied in not only the axial but also the lateral directions, which requires precise control of simultaneous two-directional loading. In addition, it has been reported by Yoshida et al. [9] and Gupta et al. [3] that conventional measurement of axial strain with external transducers would underestimate the resilient modulus. Such underestimation is due mainly to the effects of bedding error at the top and bottom ends of the specimen [8]. Therefore, it would be also required to add transducers for internal or local deformation measurements that are free from the effects of bedding error to conventional triaxial apparatus.

On the other hand, as schematically shown in Fig. 1, cyclic one-dimensional loading tests on a specimen with its lateral deformation restrained by a mold would be much easier to conduct in the laboratory. Due to their simplicity in operation, they may be employed for comparative studies on the use of nontraditional materials which have not been utilized in the field of geotechnical engineering, as is the case with the material employed in this study. Like the triaxial test results, however, the test results based on external deformation measurement would be affected by the bedding error, and it is technically difficult to make use of internal or local deformation measurements due to the existence of the mold.

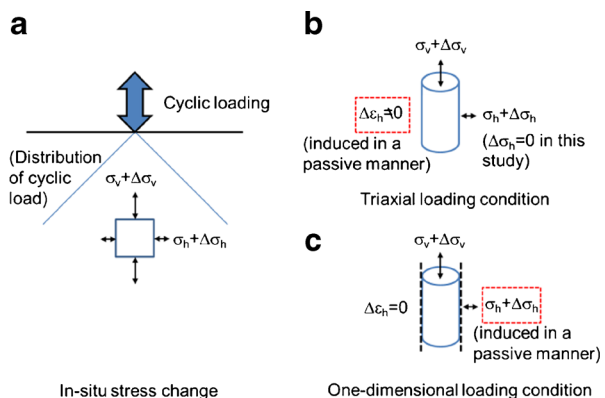
In view of the above, in the present study, it was attempted to evaluate and correct the effects of bedding error on the results from cyclic one-dimensional loading tests by employing specimens with varied heights. Comparison with the results from relevant triaxial tests employing local deformation measurement was also made.

### Tested Materials

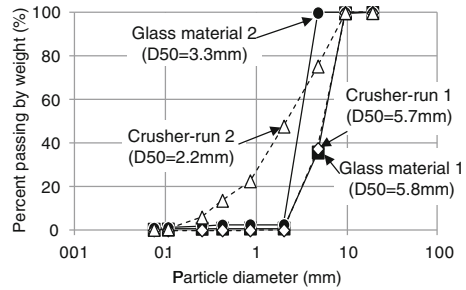
Two types of glass materials and two types of gravelly soils were tested. The former is made from recycled glass bottles as granular materials that are equivalent to natural sands and gravels [4–6], and the latter is manufactured by crushing stones or rock masses (called as “crusher-run” herein) as geomaterials for constructing embankment, base course, and foundation.

Figure 2 shows their particle size distributions. One of the glass materials (glass material 1) consisted of particles with diameters ranging from 2.0 to 9.5 mm. For

**Fig. 1** Illustration of in situ stress change and triaxial and one-dimensional loading conditions



**Fig. 2** Particle size distributions of tested materials



comparison purpose, one of the crusher-runs (crusher-run 1) was adjusted to have a gradation that is similar to the above glass material, while the other glass material (glass material 2) was prepared by sieving it with a mesh having an aperture of 4.75 mm. In addition, the other crusher-run (crusher-run 2) was prepared to have much wider gradation range, while keeping the maximum grain size at 9.5 mm. In Fig. 2, the values of the mean diameter  $D_{50}$  for each of the tested materials are also shown, which are in the range of 2.2 to 5.8 mm.

In this study, the glass materials and the crusher-runs were tested under air-dried condition with initial water contents of 0.4 and 0.6 %, respectively.

## Test Apparatus and Procedures

Figure 3 shows the general setup of the test apparatus. A cylindrical metal mold having an inner diameter of 150 mm and a height of 125 mm (without the collar) was used to confine the lateral deformation of the specimens. In order to apply cyclic vertical loading to the specimen through a metal top platen having a diameter of 148 mm, a pneumatic loading system was employed, which was controlled with an electro-pneumatic transducer connected to a function generator.

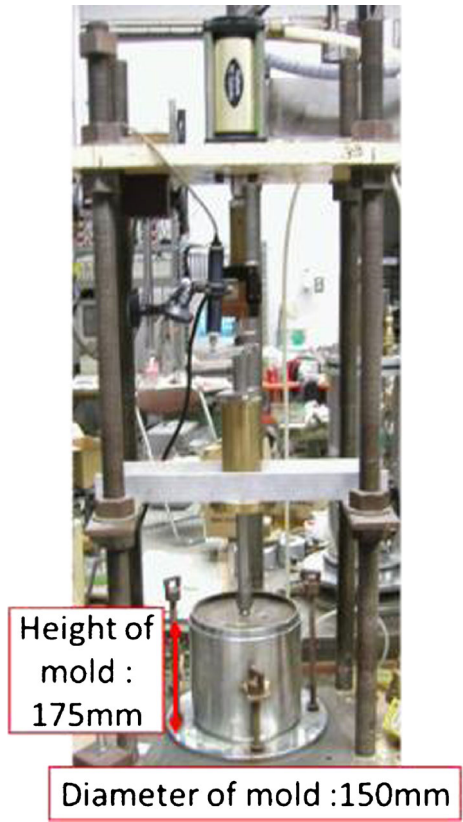
The vertical load was measured with a load cell installed above the loading plate, which is free from the friction effects at the bearings of the loading shaft, and the vertical deformation of the specimen was measured externally with a displacement transducer attached to the loading shaft.

It is to be noted that, although the results from one-dimensional loading tests are affected by the side friction at the interface between the inner surface of the mold and the specimen, no correction could be made in this study due to the technical difficulties in evaluating its effect quantitatively.

Specimens with different initial heights in the range of 25 to 125 mm were prepared by compaction in one to five layers (i.e., with a vertical lift of 25 mm), respectively, under the conditions shown in Table 1.

The initial density  $\rho_0$  of the glass material 1 was adjusted to 1.45 g/cm<sup>3</sup>, which corresponds to be 95 % of the maximum density obtained in the modified Procter compaction tests. The  $\rho_0$  value (1.43 g/cm<sup>3</sup>) of the glass material 2 was similar to the above, while its compaction tests could not be executed due to lack of available quantity. By conducting sieve analyses on the full amount of tested specimens of the

**Fig. 3** Apparatus for cyclic one-dimensional loading tests



glass material 1, it was confirmed that the degrees of particle crushing by the above compaction and the cyclic loading were not noticeable [6].

On the other hand, in order to avoid further particle crushing that would alter the gradation, the crusher-run 1 was compacted to lesser extents with a lower  $\rho_0$  value equal to  $1.31 \text{ g/cm}^3$ . It was also the case with the compaction of the crusher-run 2, while the highest  $\rho_0$  value ( $1.54 \text{ g/cm}^3$ ) among the four types of tested materials could be achieved thanks to its well-graded condition.

After applying monotonically an initial vertical stress of 20 kPa to the specimen, 30,000 cycles of vertical loading at a frequency of 0.5 Hz were performed, where the vertical stress was changed in-between 20 and 50 kPa in a sinusoidal manner. By

**Table 1** Test conditions

Tested material	Initial density, $\rho_0$ ( $\text{g/cm}^3$ )	Initial specimen height, $H$ (mm)
Glass material 1	1.45	25 <sup>a</sup> , 50 <sup>a</sup> , 75 <sup>a</sup> , 100, 125 <sup>a</sup>
Glass material 2	1.43	25, 75, 125
Crusher-run 1	1.31	25 <sup>a</sup> , 75 <sup>a</sup> , 125 <sup>a</sup>
Crusher-run 2	1.54	25, 75, 125

<sup>a</sup>Two tests were conducted under the same conditions

conducting additional tests, it was confirmed that the increase of residual displacement by cyclic loading became insignificant after the number of cycles exceeded 30,000.

## Test Results and Discussions

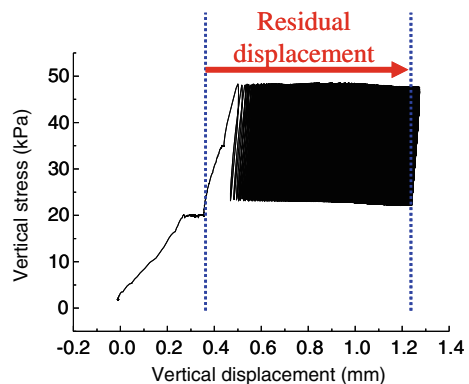
### Measured Residual Displacement

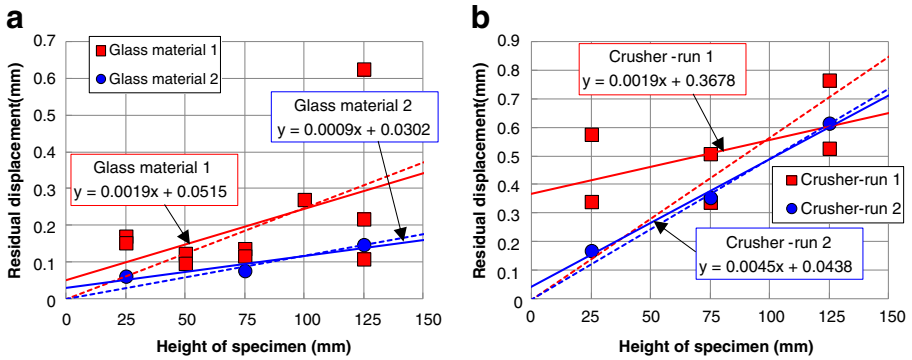
In this study, residual displacement was defined as the increment of the vertical displacement from state at the end of monotonic loading and the state after the loading of 30,000 cycles, as typically shown in Fig. 4. The vertical stress at these states were the same (20 kPa).

Figure 5a shows relationships between the residual displacement and the initial specimen height of the glass materials. A linear relationship that passes through the origin, such as those shown by dashed lines, would be expected if the overall residual vertical strain evaluated as the residual displacement normalized with the specimen height is kept constant. However, the measured relationships did not exhibit such trend. Rather, they could be approximated by straight lines with positive  $y$ -intercepts, as shown by solid lines in the figure, suggesting that the overall residual strain decreased with the specimen height. Such behavior may be explained by considering the possible effects of bedding error, as will be discussed in the next section.

It should be noted that the test results on the glass material 1 revealed larger deviations from the approximated line, in particular, with a specimen height of 125 mm. Such different extents of deviations may be linked to the difference in the particle diameter, since specimens with the same total volume but larger particles consist of smaller number of particles, resulting into larger degrees of heterogeneity. Attempts have been made to identify the source of such deviations, while the authors could not find any significant effect of slight changes in density or gradation of the specimen. Rather, the particle shape of the glass material 1, which was flatter than those of other materials tested in this study, may have induced larger variations in the thickness of the bedding error layer as will be analyzed in the next section, resulting into larger deviations in the measured residual displacements. Figure 5b shows relationships between the residual displacement and the initial specimen height of the

**Fig. 4** Typical test result and definition of residual displacement





**Fig. 5** Relationship between residual displacement and initial specimen height: **a** glass materials and **b** crusher-runs

crusher-runs. As was the case with the glass materials, the observed trends could be more reasonably approximated by solid straight lines with positive *y*-intercepts than by dashed lines with zero *y*-intercept, and larger deviations from the approximated line were observed with the crusher-run 1 that consists of larger particles. Such larger deviations may have been also affected by the lowest initial density of the specimens as listed in Table 1.

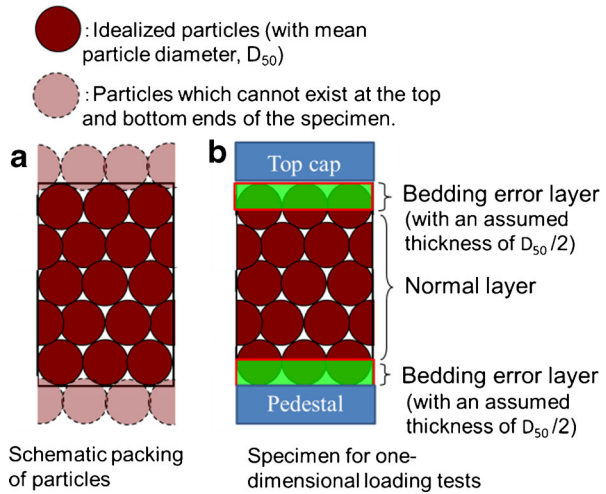
### Evaluation of Effects of Bedding Error on Residual Strain

In order to evaluate the effects of bedding error on the measured residual displacements, it was assumed that the specimen can be divided into two kinds of regions: one is a bedding error layer that corresponds to the looser zones at the top and bottom ends of the specimen as illustrated in Fig. 6, and the other is a normal layer that is free from the effects of bedding error. It was further assumed that the thickness of each of the bedding error layers, which was assumed to be half of the particle mean diameter  $D_{50}$ , does not change with the specimen height. Under this assumption, the nominal residual strain for the whole specimen would decrease with the specimen height, since the contribution of the larger deformation of the bedding error layers would become smaller.

Based on the approximated relationships shown in Fig. 5, the residual displacement of the bedding error layers and the residual strain of the normal layer were evaluated, respectively, from the *y*-intercepts and the slope. In addition, by assuming for simplicity that the thickness of each of the bedding error layers is equal to half of the particle mean diameter, the residual strain of the bedding error layers was also estimated.

As summarized in Table 2, the estimated residual strains of the bedding error layers and the normal layer for the four types of tested materials were on the order of 1 % (in-between 0.9 and 7.2 %) and 0.1 % (in-between 0.09 and 0.45 %), respectively. Considering the deviation of the measured data from the approximated lines, it would be preferred to make such estimation on a statistical basis, while it was not attempted in this study due to insufficient number of test data.

**Fig. 6** Installation of bedding error layers and normal layer



### Evaluation of Effects of Bedding Error on Constrained Modulus

Based on the same assumptions as were made in the previous section, the compatibility condition in terms of the specimen deformation during cyclic loading can be obtained as

$$\frac{\Delta\sigma}{M_1}D_{50} + \frac{\Delta\sigma}{M_2}(H-D_{50}) = \frac{\Delta\sigma}{M_0}H \tag{1}$$

where  $M_1$  is the constrained modulus of the bedding error layer,  $M_2$  is the constrained modulus of the normal layer,  $M_0$  is the nominal value of the constrained modulus evaluated in a conventional manner for the whole specimen height,  $H$  is the height of the specimen,  $D_{50}$  is the particle mean diameter, and  $\Delta\sigma$  is the vertical stress increment applied to the specimen. It can be rewritten as

$$\frac{1}{M_0} = \left( \frac{1}{M_1} - \frac{1}{M_2} \right) * \frac{D_{50}}{H} + \frac{1}{M_2} \tag{2}$$

**Table 2** Nominal residual strain for whole layers and estimated results for bedding error layers and normal layer

Tested material	Whole layers Nominal residual strain (%)	Bedding error layers		Normal layer Residual strain (%)
		Residual displacement (mm)	Residual strain (%)	
Glass material 1	0.09 to 0.69	0.05	0.9	0.19
Glass material 2	0.10 to 0.24	0.03	1.2	0.09
Crusher-run 1	0.42 to 2.33	0.37	7.2	0.19
Crusher-run 2	0.48 to 0.68	0.04	2.5	0.45

Based on Eq. (2), the values of  $M_1$  and  $M_2$  can be evaluated from the relationship between  $1/M_0$  and  $1/H$  for the test results on specimens with different heights.

From the stress–strain relationship measured during cyclic loading, as typically shown in Fig. 7, the nominal constrained modulus  $M_{0,i}$  at the  $i$ th cycle was obtained by fitting it with a straight line. In this study, a representative  $M_0$  value is evaluated as

$$M_0 = \frac{M_{0,10} + M_{0,100} + M_{0,1000} + M_{0,10000} + M_{0,20000} + M_{0,30000}}{6} \tag{3}$$

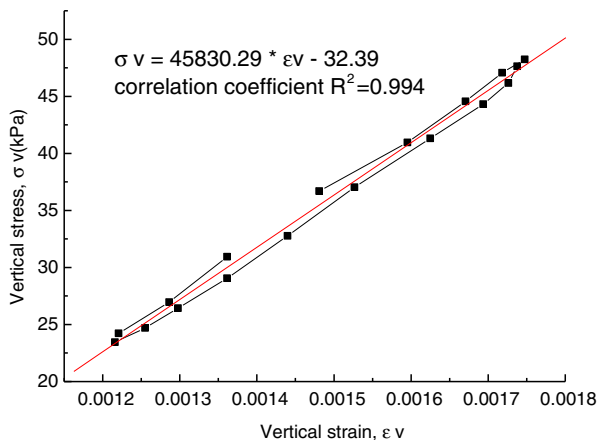
It should be noted that the  $M_{0,i}$  values did not exhibit any clear tendency of increase or decrease with the number of cycles.

Figure 8a, b shows the relationships between  $1/M_0$  and  $1/H$ , respectively, for the grass materials and the crusher-runs. The observed values of  $1/M_0$  were not constant but increased with the values of  $1/H$  (i.e., the  $M_0$  values decreased with the reduction in  $H$ ). Such tendency is consistent with the trend as formulated by Eq. (2). By making approximation of the observed relationships with straight lines, therefore, the values of  $M_1$  and  $M_2$  were estimated based on Eq. (2).

Table 3 summarizes the estimated results. The constrained moduli of the normal layer were on the order of 100 MPa (in-between 150 and 330 MPa), except for the results on the crusher-run 1 that exhibited a negative  $M_2$  value. In general, they were larger than the nominal  $M_0$  values as also listed in Table 3. On the other hand, the constrained moduli of the bedding error layer,  $M_2$ , were on the order of several megapascals (in-between 2.1 and 5.3 MPa), which were significantly lower than those of the normal layer.

The reason for the unsuccessful estimation of the  $M_2$  value of the crusher-run 1 is not known to the authors, but it may be linked to its relatively larger particles that may have affected the degrees of heterogeneity, as discussed in the earlier section. This may also suggest a limitation of the simplified assumption made in this study. In addition, it should be noted that the above estimation results on the  $M_2$  values are directly affected by the assumed thickness of the bedding error layer, on which future quantitative studies are required.

Fig. 7 Typical stress–strain relationship during cyclic loading





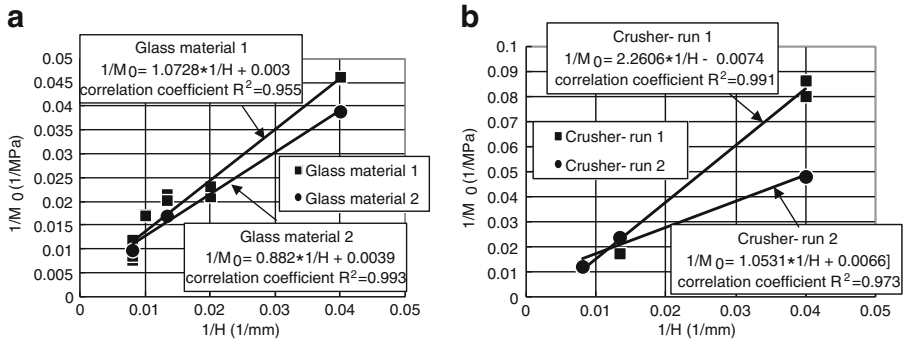


**Fig. 8** Relationship between  $1/M_0$  and  $1/H$ : **a** glass materials and **b** crusher-runs

**Comparison with Triaxial Test Results**

Triaxial Test Procedures and Conditions

Triaxial tests were performed on the glass material 1. A cylindrical specimen having a diameter of 100 mm and an initial height of about 100 or 200 mm was prepared by compacting it in a mold to the same density as employed in the one-dimensional cyclic loading tests.

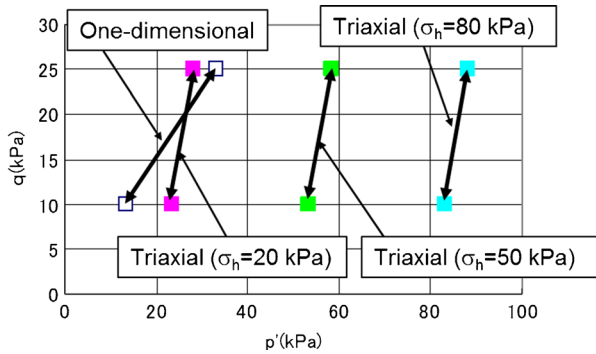
After consolidating the specimen isotropically to a confining stress of 20 kPa, the deviator stress was initially raised to 10 kPa, which was then cyclically changed in-between 10 and 25 kPa. Since the response of the motor-driven axial loading system [7] employed for this study was not sufficiently quick, the number of the cyclic loading had to be limited to 3,000, while it still took longer than 30,000 s for completing the cyclic loading (i.e., the average frequency of cyclic loading was smaller than 0.1 Hz). In this study, possible effects of the cyclic loading frequency were not considered.

Figure 9 compares the stress paths during cyclic loading in the triaxial and the one-dimensional cyclic loading tests, where the coefficient of earth pressure at rest ( $\sigma_h/\sigma_v$ ) during the one-dimensional tests was assumed to be kept at 0.5. For further comparison, additional cyclic triaxial tests were also conducted at higher confining stresses of 50 and 80 kPa, while maintaining the other test conditions.

**Table 3** Nominal constrained modulus for whole layers and estimated results for bedding error layers and normal layer

Tested material	Whole layers	Bedding error layers	Normal layer
	Nominal constrained modulus, $M_0$ (MPa)	Estimated constrained modulus, $M_1$ (MPa)	Estimated constrained modulus, $M_2$ (MPa)
Glass material 1	$2.2 \times 10^1$ to $1.3 \times 10^2$	5.3	$3.3 \times 10^2$
Glass material 2	$2.6 \times 10^1$ to $1.0 \times 10^2$	3.7	$2.6 \times 10^2$
Crusher-run 1	$1.2 \times 10^1$ to $8.5 \times 10^1$	2.6	$-1.4 \times 10^2$
Crusher-run 2	$2.1 \times 10^1$ to $8.2 \times 10^1$	2.1	$1.5 \times 10^2$

**Fig. 9** Stress paths during cyclic loading in triaxial and one-dimensional cyclic loading tests

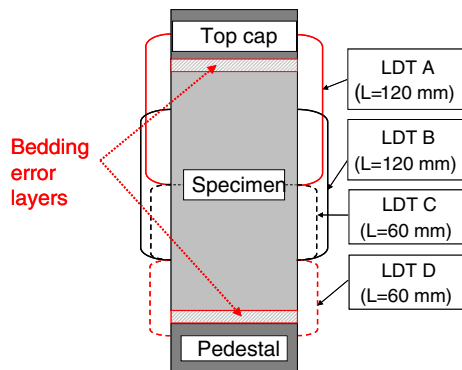


In the above additional tests on specimens with an initial height of 200 mm, as schematically shown in Fig. 10, four pairs of local deformation transducers [2] were installed at their side surface, which will be referred to as LDTs A through D. Figure 11 shows typical results from axial strain measurements evaluated by the four pairs of LDTs and those from external measurement. LDTs could not be used at a confining stress of 20 kPa, due to the technical difficulties in supporting them without disturbing their fixing points at such low confining stress.

Triaxial Test Results on Residual Deformation and Discussions

Figure 12 shows relationships between the residual axial displacement by external measurement after the 3,000 cycles and the initial specimen height, *H*. By employing the same procedures as mentioned on the cyclic one-dimensional loading test results, the residual strains in the bedding error and normal layers are estimated as summarized in Table 4. It should be noted that some experimental results as plotted in hollow symbols with horizontal arrow in Fig. 12 had to be excluded from the analysis, since they yielded extremely small residual displacements as compared to other test results. The reason for such discrepancy is not known to the authors, while it may be due possibly to the effects of heterogeneity of specimens consisting of relatively larger particles (such as the case with the specimens of crusher-run 1 for one-dimensional loading tests, as discussed previously).

**Fig. 10** Installation of four pairs of LDTs on specimens with a height of 200 mm



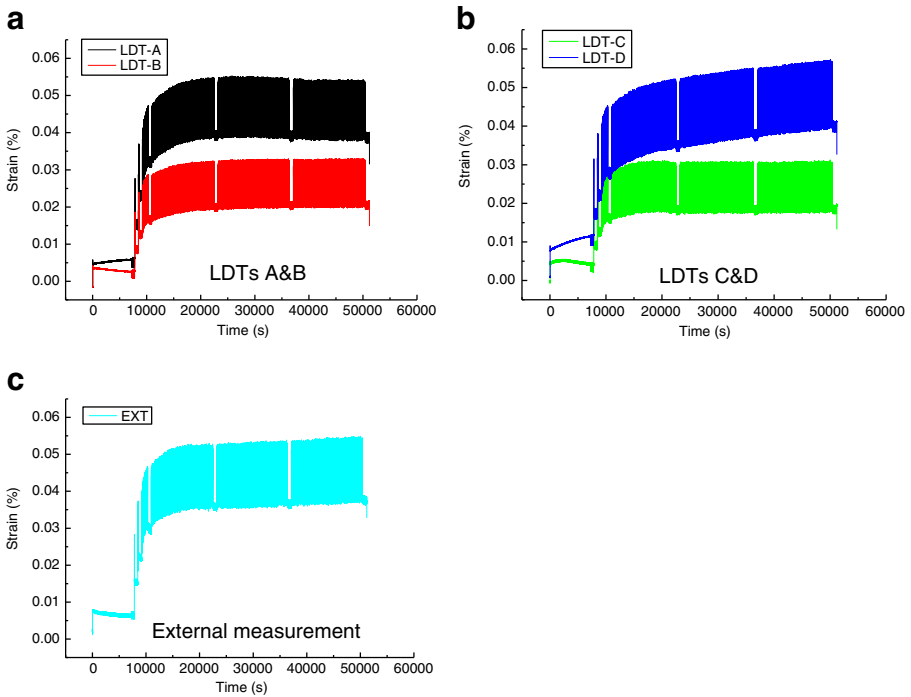


**Fig. 11** Typical results from local and external axial strain measurements

For comparison, the residual strains evaluated with LDTs A through D are also shown in Table 4. It can be seen that the residual strains with LDTs B and C, which would be free from the effects of the bedding error (Fig. 9), were in the range of 0.012 to 0.019 % and 0.001 to 0.015 %, respectively. The order of these values were, in general, 0.01 %, which was consistent with the estimated residual strains based on external measurement with varied specimen heights (0.023 and 0.014 %, respectively, at confining stresses of 50 and 80 kPa).

The estimation based on external measurement yielded a higher residual strain of 0.057 % after 3,000 cycles at a confining stress of 20 kPa, due possibly to the effects of lower confining stress that would enhance the effect of bedding error. This value would increase more with the number of cycles, approaching the

**Fig. 12** Relationship between externally measured residual axial displacement and initial specimen height

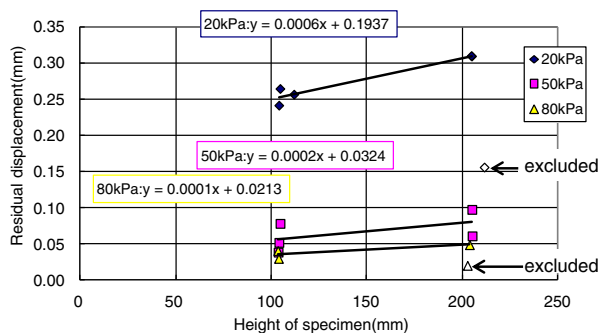


**Table 4** Residual strains estimated from external measurements and measured locally with LDTs

Tested material	Confining stress (kPa)	Estimated from external measurements (%)		Measured locally with LDTs (%)			
		Bedding error layers	Normal layer	A	B	C	D
Glass material 1	20	3.3	0.057	–	–	–	–
	50	0.56	0.023	0.034	0.019	0.015	0.030
	80	0.37	0.014	0.013 <sup>a</sup>	0.012 <sup>a</sup>	0.001 <sup>a</sup>	0.018 <sup>a</sup>

<sup>a</sup> Average of two test results

order of 0.1 %, which is in the same order as the estimated result shown in Table 2 (0.19 % after 30,000 cycles) based on the cyclic one-dimensional loading tests.

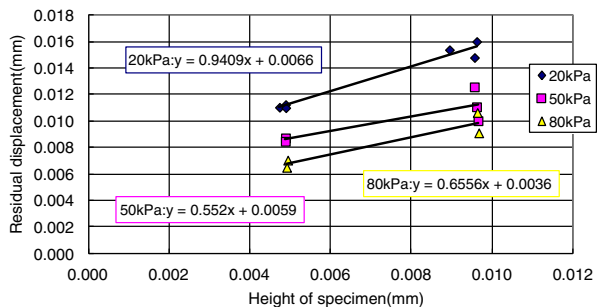
Triaxial Test Results on Equivalent Young’s Modulus and Discussions

Figure 13 shows the relationships between  $1/E_0$  and  $1/H$ , where  $E_0$  denotes the nominal equivalent Young’s modulus based on external measurement during cyclic loading, which was evaluated in a manner similar to  $M_0$  as mentioned previously on the one-dimensional loading test results. Based on these relationships, the values of Young’s moduli in the bedding error layer ( $E_1$ ) and the normal layer ( $E_2$ ) were estimated as summarized in Table 5. The  $E_2$  values were on the order of 100 MPa, which increased with the confining stress. On the other hand, the  $E_1$  values were on the order of several megapascals and were significantly smaller than the  $E_2$  values by a factor of about 20 to 30.

In Table 5, results from local measurements using LDTs are also shown. The values of Young’s moduli evaluated by LDTs B and C that would be free from the effect of the bedding error were consistent with those estimated based on the external measurement as mentioned above. On the other hand, the values of Young’s moduli evaluated by LDTs A and D that would be affected by the bedding error (Fig. 9) were, in general, smaller.

Under simplified assumption of isotropic linear elasticity, the constrained modulus can be evaluated from the Young’s modulus as

**Fig. 13** Relationship between  $1/E_0$  and  $1/H$



**Table 5** Equivalent Young's moduli estimated from external measurements and measured locally with LDTs

Tested material	Confining stress (kPa)	Estimated from external measurements (MPa)		Measured locally with LDTs (MPa)			
		Bedding error layers, $E_1$	Normal layer, $E_2$	A	B	C	D
Glass material 1	20	5.9	$1.5 \times 10^2$	–	–	–	–
	50	9.9	$1.7 \times 10^2$	140	175	176	126
	80	8.6	$2.8 \times 10^2$	176 <sup>a</sup>	200 <sup>a</sup>	177 <sup>a</sup>	156 <sup>a</sup>

<sup>a</sup> Average of two test results

$$M = \frac{1-\nu}{(1+\nu)(1-2\nu)}E \quad (4)$$

where  $\nu$  is the Poisson's ratio. Due to lack of experimental data, the  $\nu$  value was assumed to be within a range of 0.1 and 0.3 in this study. Then the values of the ratio  $M/E$  became 1.02 and 1.35, respectively, for  $\nu=0.1$  and 0.3. As a result, the estimated Young's moduli at a confining stress of 20 kPa (i.e.,  $E_1=5.9$  MPa and  $E_2=150$  MPa) yielded the range of constrained moduli of the bedding error layers and the normal layer, respectively, as  $M_1=6.0$  to 8.0 MPa and  $M_2=150$  to 200 MPa. These ranges were consistent with the values of  $M_1$  (5.3 MPa) and  $M_2$  (330 MPa) that were estimated based on the cyclic one-dimensional loading tests, as has been described previously on the one-dimensional loading test results.

## Conclusions

The results from the cyclic one-dimensional loading tests on compacted specimens with varied heights, which were made from four types of granular materials, can be summarized as follows:

- 1 The residual displacements of specimens that were measured with external displacement transducer were not in proportion to the specimen height. By extrapolating the test results, it was estimated that, even if the specimen height approaches to 0, there would be a nonzero but positive residual displacement.
- 2 By assuming that the top and bottom ends of the specimen are affected by bedding error, it was attempted to estimate the residual strain of the normal layer that is free from the effect of the bedding error. As a result, the residual strains of the tested materials were on the order of 0.1 %. On the other hand, much higher residual strains were estimated for the layers affected by the bedding error.
- 3 By adapting the same assumption as above, the constrained modulus of the specimen that is free from the effect of the bedding error was estimated. The constrained moduli of the three types of the tested materials were found to be on the order of 100 MPa, which were much larger than the nominal values of the constrained modulus that were evaluated in a conventional manner. However,

reasonable estimation could not be made with the other type of the tested material consisting of relatively large particles, suggesting a limitation of the simplified assumption.

- 4 The above values of the residual strain of the normal layer and the constrained moduli were consistent with the results from relevant triaxial tests, which were conducted on one type of the tested material.

**Acknowledgments** The authors wish to thank Glass Resourcing Co., Ltd., Japan, for providing the glass materials employed in this study.

## References

1. Chummuneerat, S., Jitsangiam, P., Nikraz, H.: Mechanical characteristics of hydrated cement treated crushed rock base for western australian road base, *Advances in Transportation Geotechnics II*, Miura et al. (eds.), CRC Press, 296–301 (2012)
2. Goto, S., Tatsuoka, F., Shibuya, S., Kim, Y.-S., Sato, T.: A simple gauge for local small strain measurements in the laboratory. *Soils Found* **31**(1), 169–180 (1991)
3. Gupta, S., Ranaivoson, A., Edil, T., Benson, C., Sawangsuriya, A.: Pavement Design Using Unsaturated Soil Technology, Report No. MN/RC-2007-11, Final Research Report submitted to Minnesota Department of Transportation, University of Minnesota, Minneapolis, <http://www.cts.umn.edu/Publications/ResearchReports/reportdetail.html?id=1266>, 69–70 (2007)
4. Mikami, T., Koseki, J., Sato, T., Yajima, C.: Study on use of granular materials made from recycled glass bottles as a countermeasure against earthquake-induced uplift of underground pipes, *Earthquake Geotechnical Engineering Satellite Conference. 17th International Conference on Soil Mechanics and Geotechnical Engineering*, Alexandria, Egypt (2009). CD-ROM
5. Mikami, T., Koseki, J., Sato, T., Yajima, C.: Effects of geogrids on compaction of granular materials made from recycled glass bottles in backfilling works, pp. 1413–1416. *Proc. of 9th International Conference on Geosynthetics*, Brazil (2010)
6. Mikami, T., Koseki, J., Sato, T.: Experimental study on deformation characteristics of granular materials made from recycled glass bottles under traffic loading, *Advances in Transportation Geotechnics II*, Miura et al. (eds.), CRC Press, 340–345 (2012)
7. Santucci de Magistris, F., Koseki, J., Amaya, M., Hamaya, S., Sato, T., Tatsuoka, F.: A triaxial testing system to evaluate stress–strain behaviour of soils for wide range of strain and strain rate. *Geotech Test J* **22**, 44–60 (1999)
8. Tatsuoka, F. and Shibuya, S.: Deformation characteristics of soils and rocks from field and laboratory tests, Keynote Lecture for Session No.1, *Proc. of the 9th Asian Regional Conf. on SMFE*, Bangkok, II, 101–170 (1991)
9. Yoshida, N., Sugisako, Y., Nakamura, H., Hirotsu, E.: Resilient modulus of hydraulic mechanically stabilized slag base-course material, *Deformation Characteristics of Geomaterials*, Di Benedetto et al. (eds.), Balkema, 293–298 (2003)
10. Vuong, B.T.: Precision studies of resilient modulus and permanent strain testing, *Unbound Granular Materials*, Gomes Correia (ed.), Balkema, 63–83 (1999)